

Anderson Localization and Mobility Edges in Ruby

J. Koo,* L. R. Walker, and S. Geschwind
Bell Laboratories, Murray Hill, New Jersey 07974
 (Received 17 September 1975)

When the R_1 line in ruby is swept with a tunable laser from the center to the wings, the ratio of trap emission to R_1 emission remains constant up to a point in the line where it suddenly drops to a lower constant value out to the wings. We suggest that this break corresponds to mobility edges separating delocalized states in the central region from "localized" states beyond this break.

In ruby, the Cr^{3+} ion substitutes randomly for the Al^{3+} in the Al_2O_3 lattice. The uncorrelated random components of the crystal field at different Cr^{3+} sites give rise to a distribution of energies of width 2Γ for the ${}^4A_2 \rightarrow \bar{E}({}^2E)$ transition (R_1 line). 2Γ is observed as the limiting width of the R_1 absorption line at sufficiently low temperatures ($\lesssim 20$ K) such that phonon-broadening effects¹ are negligible and is of the order of 1 cm^{-1} in our samples. An interaction $V_{ii'}(r_{ii'})$ transfers excitation from an ion in the excited $\bar{E}({}^2E)$ state at site i to an ion in the 4A_2 ground state at site i' . According to Anderson's ideas,² if $V_{ii'}$ falls off faster than $1/r_{ii'}^3$, there is a critical concentration of Cr^{3+} ions, c_{crit} , below which there is no diffusion and the excitation is spatially localized. Lyo³ using an anisotropic exchange interaction for $V_{ii'}$, as suggested by Birgeneau⁴ for ruby, has calculated c_{crit} to be about 0.3% Cr^{3+} .

Mott⁵ and others^{6,7} have extended Anderson's remarkable result to $c > c_{\text{crit}}$. Their results imply that above c_{crit} , mobility edges, $\pm E_c$ from line center (Fig. 1), should separate delocalized or excitonic $\bar{E}({}^2E)$ states in the central region of the R_1 line from localized states in the wings. E_c should increase rapidly as c increases. An extensive literature⁸ deals with this Anderson transition in the context of the metal-insulator transition, where the existence of mobility edges is deduced from an average transport property such as conductivity. However, very few if any experiments exist which have *selectively* probed the states in the bandwidth 2Γ to discriminate between localized and delocalized states. We report here on such an experiment in ruby.

In our experiment, a cw ruby laser tuned by magnetic field and temperature, and pumped by an argon-ion laser, excites different regions of the R_1 absorption line. The laser linewidth is a fraction of the R_1 linewidth (Fig. 1). Excitation in single Cr^{3+} ions may also be transferred to

exchange-coupled Cr^{3+} pairs, which act as traps several hundred reciprocal centimeters below the single-ion \bar{E} level. Imbusch⁹ first indicated that emission from these traps is enhanced by energy migration among single ions which brings the excitation closer to the trap. Thus, if we excite in the region of the R_1 line where the single ions are localized, trap emission will be impeded compared to excitation in the central region. We have chosen the fluorescence of the trap at 7009 \AA (N_2 line) as our monitor of localized versus delocalized \bar{E} states. For $c > c_{\text{crit}}$, the N_2/R_1 emission intensity ratio should drop from one constant value to a lower one as the laser is swept from the R_1 line center to the wings through the mobility edge.

To avoid reabsorption of R_1 light, we used single-crystal ruby samples of micron-size particles deposited in a single layer on a glass slide, or platelets < 0.001 in. thick. Samples studied ranged in concentration from 0.05 to 1.4%. All measurements were taken at a temperature of ~ 2 K.

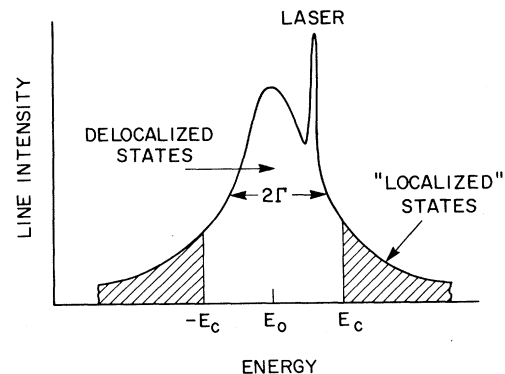


FIG. 1. Schematic division of inhomogeneously broadened line, above the critical concentration for an Anderson transition, into regions of "localized" and delocalized states. Laser light is used to excite these states selectively.

Besides feeding of the traps by excited single ions, one may have direct excitation into some excited state of the trap by the R_1 laser light itself. As the radiative lifetime of the traps is $\tau_P = 1$ msec and that of the single ions is $\tau_R = 3.6$ msec, the trap emission associated with this direct excitation may be essentially eliminated by starting the measurement of the N_2/R_1 emissions at a time $t_0 = 5$ msec after shutoff of the laser excitation.

The specimen was illuminated by the ruby laser for 5 msec by means of a mechanical chopper wheel. This was followed by a delay, $t_0 = 5$ msec, after which the N_2 and R_1 photon counts in the next 20-msec interval were integrated. This cycle was repeated at 20 cycles per second for a few minutes and the ratio of the accumulated-trap to single-ion counts, which we call T/S , was recorded as a function of the position of the excitation from the R_1 line center. The results are plotted in Fig. 2 for samples of three different concentrations with T/S normalized to unity at line center and the position from line center normalized to the half-width Γ for each particular sample. We suggest that the region of constant T/S in the central portion of the line corresponds to delocalized or excitoniclike states and the point in each line where the T/S ratio drops marks the mobility edge separating delocalized from localized states. The observed motion of the position of the edges versus c is such that even if the breaks were perfectly sharp, a reasonable macroscopic inhomogeneity in c of $\sim 10\%$

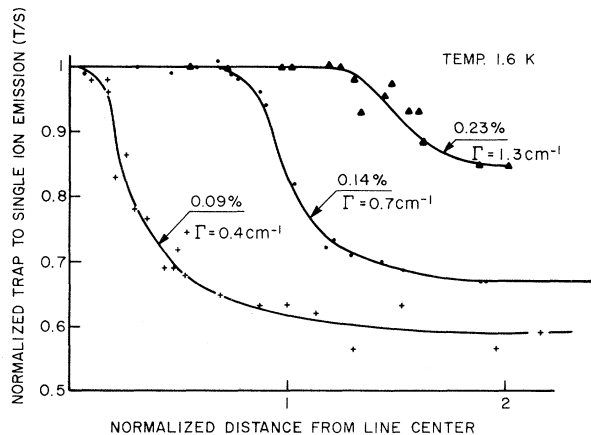


FIG. 2. Normalized trap (N_2 line) to single-ion emission (R_1 line) in ruby as a function of laser excitation in different regions of the R_1 line. The observed breaks suggest mobility edges separating delocalized states in the central region from the localized states beyond the break.

would smear them to the extent seen.

In the central region diffusion is governed by the short-range anisotropic exchange and the states are strongly delocalized. The mobility edges mark the point at which this diffusion is inhibited. However, beyond the edges, diffusion persists from the electric dipole interaction,² $V_{ii'} \sim 1/r_{ii'}^3$, which is orders of magnitude less than the anisotropic exchange for the concentrations studied. The states are now relatively localized, but since the single-ion-single-ion transport remains, as will be seen, fast compared to other rates, the observed breaks in T/S are small.

To stimulate localization in a tractable model we assume that there is a term in the rate equation for the single-ion excitation at site i , n_i , of the form $-D(n_i - \langle n_i \rangle)$, where $\langle n_i \rangle$ is the instantaneous spatial average of n_i . D serves as a measure of the localization, taking on a value D_c at the center of the line and a very much smaller value D_w in the wings. This description of the single-ion-single-ion transport of excitation is plausible if D exceeds all other relevant rates in the problem. An analysis of the data in terms of this model implies that, even in the wings, D satisfies this condition. The model is also formally correct for strict localization ($D=0$). However, in this case the predicted ratio $(T/S)_{D_w}/(T/S)_{D_c}$ is an order of magnitude less than is found and so we reject such small values of D . At laser pump levels insufficient to saturate the traps, the rate equations for n_i and for p_j , the trap excitation probability at site j , are now taken to be

$$\dot{n}_i = -\frac{n_i}{\tau_R} - n_i \sum_j y_j w_{ij} + D \left(\frac{\sum_i x_i n_i}{\sum_i x_i} - n_i \right) + F(t)(1 - 2n_i), \quad (1)$$

$$\dot{p}_j = -p_j/\tau_P + \sum_i x_i n_i w_{ij}. \quad (2)$$

$F(t)$ is the laser pump rate, constant during the pumping and zero thereafter; x_i and y_j equal 1 (or 0) when there is (or is not) a Cr^{3+} ion or trap, respectively, at site i or j ; and w_{ij} is the rate at which an excited Cr^{3+} at i decays by the transfer of energy to a trap at site j . At a temperature of 2 K there is no feeding of the single ions by the traps. The direct pump contribution to p_j is ignored since this has substantially vanished at t_0 when the counting starts, as indicated earlier.

Equations (1) and (2) may be solved exactly for a given set of x_i and y_j . The integrated single-ion count, $S = (1/\tau_R) \int_{t_0}^{\infty} \langle \sum_i x_i n_i(t) \rangle dt$, and the in-

tegrated trap count, $T = (1/\tau_R) \int_{t_0}^{\infty} \langle \langle \sum_j y_j p_j(t) \rangle \rangle dt$, where $\langle \langle \dots \rangle \rangle$ indicates an ensemble average, may then be written down. $\langle \langle x_i \rangle \rangle = c$ and $\langle \langle y_i \rangle \rangle = d$, the trap concentration (where in fact $d = \frac{3}{2}c^2$).

For small c and d , it is sufficient to calculate S to first order in c and zero order in d , and T to first order in c and d . The expression for T/S now simplifies for significant values of D , and becomes

$$\frac{T}{S} = d\tau_R \sum_j \frac{D w_{0j}}{D + w_{0j}} \times \frac{\tau_R - \tau_P \exp[-t_0(\tau_P^{-1} - \tau_R^{-1})]}{\tau_R - \tau_P}. \quad (3)$$

The summation runs over the complete lattice, excluding those neighbors of a given trap (whose center is at 0) which are so perturbed by the pair that they no longer appear in the spectrum of the R_1 line. These were taken to be the first to fourth neighbors of *either* ion in the pair. w_{0j} is taken to be proportional to the square of the anisotropic exchange^{3,4} and may be expressed as $A \exp(-2\alpha r_{0j})$, where we estimate $\alpha \approx 1.03 \text{ \AA}^{-1}$. The ratio of T/S in the localized regime ($D = D_w$) to T/S in the delocalized regime ($D = D_c$) is now

$$\frac{(T/S)_{D_w}}{(T/S)_{D_c}} = \frac{\sum_j D_w w_{0j} / (D_w + w_{0j})}{\sum_j D_c w_{0j} / (D_c + w_{0j})}. \quad (4)$$

Assuming a particular value for D_c , we use Eq. (3) and the observed values of T/S at the line center to fix the amplitude A in w_{0j} . Equation (4) may then be used with the experimental T/S values to find corresponding D_w values. D_c should be of the order of some representative single-ion-single-ion transfer rate associated with anisotropic exchange which Birgeneau⁴ has estimated to be of the order of 10^7 sec^{-1} in 1% ruby. Only $D_c / \sum_j w_{0j}$ is determined from our data, but requirements upon this ratio can be used to fix D_c . Since the single-ion to trap energy transfer rate $\sim c \sum_j w_{0j}$ must be phonon assisted,^{4,9} it will be down by approximately a factor of 10^3 from D_c . Thus, from the experimental value $T/S = 15.9 \times 10^{-3}$ for $c = 0.23 \times 10^{-2}$, the requirement $D_c / c \sum_j w_{0j} > 10^3$ is only satisfied for $D_c > 10^6$, which is not inconsistent with the earlier estimates.^{4,9} Contrary claims that D_c is essentially zero are at variance with our observation of the mobility edges.^{10,11}

In Table I are listed the values of D_w derived from the experimental T/S values using Eqs. (3) and (4). We find that any value of $D_c > 10^6$ yields the same results for D_w as for $D_c = 10^6$. The derived values of D_w increase with c as expected

TABLE I. $(T/S)_{D_c}$, $(T/S)_{D_w}/(T/S)_{D_c}$, and τ_R' for samples of different Cr^{3+} concentration, c . The values of D_w listed pertain to $D_c \geq 10^6 \text{ sec}^{-1}$. Quoted c 's are accurate to 10%.

c (%)	$(T/S)_{D_c}$	τ_R' (msec)	$\frac{(T/S)_{D_w}}{(T/S)_{D_c}}$	D_w (sec^{-1})
1.4	...	<2	No break	...
0.5	...	3.4	No break	...
0.23	15.9×10^{-3}	3.6	0.85	1.31×10^5
0.14	4.6×10^{-3}	3.6	0.67	4.54×10^4
0.09	2×10^{-3}	3.6	0.59	3.07×10^4
0.05	...	3.6	No break	...

and the variation goes almost as c^2 or as $\langle 1/r_{ii'}^6 \rangle$, which is suggestive of a dipolar dependence. However, the exact behavior of dipolar diffusion in the Anderson model is rather complicated. The values of D_w derived are larger than suggested by previous estimates.^{4,9} Note the very narrow range of c over which the mobility edges may be observed.¹² No mobility edge was found for $c = 5 \times 10^{-4}$ and our data in Fig. 2 suggest that the Anderson transition occurs at $c \approx 0.8 \times 10^{-3}$. At higher c the break becomes smaller, moves towards the wings, and is obscured by reabsorption.

If τ_R' is the effective single-ion relaxation time one may derive a relation between measured quantities:

$$\tau_R' = \tau_R \left(1 + b \frac{T}{S} \frac{\tau_R - \tau_P}{\tau_R - \tau_P \exp[-t_0(\tau_P^{-1} - \tau_R^{-1})]} \right)^{-1}, \quad (5)$$

where b (~ 3) takes account of relaxation to other types of traps in addition to the monitored fourth-nearest neighbors. When the experimentally observed values of T/S are inserted in Eq. (5), the second term in the brackets is seen to produce an unobservable correction to τ_R up to $c = 2.3 \times 10^{-3}$ and indeed none is observed within the experimental error of a few percent in τ_R . For $c = 14 \times 10^{-3}$ the predicted τ_R' is 1.6 msec but because of reabsorption $\tau_R' = 2.0$ msec is observed. These effects for larger c , even in the fine powders, precluded the observation of the mobility edges and the Anderson transition by the measurement of different τ_R' 's in the wings and center of the line.¹³ Finally, the spatial delocalization we see need not necessarily imply spectral diffusion.¹⁴

We thank M. D. Sturge and P. W. Anderson for helpful discussions.

*Now at Western Electric Engineering Research Center, Princeton, N. J. 08540.

¹D. E. McCumber and M. D. Sturge, *J. Appl. Phys.* **34**, 1682 (1963).

²P. W. Anderson, *Phys. Rev.* **109**, 1492 (1958), and *Comments Solid State Phys.* **2**, 193 (1970).

³S. K. Lyo, *Phys. Rev. B* **3**, 3331 (1971).

⁴R. J. Birgeneau, *J. Chem. Phys.* **50**, 4282 (1969).

⁵N. F. Mott, *Advan. Phys.* **16**, 49 (1967).

⁶Morrel H. Cohen, H. Fritzsche, and S. R. Ovshinsky,

Phys. Rev. Lett. **22**, 1065 (1969).

⁷E. N. Economou and Morrel H. Cohen, *Phys. Rev. B* **5**, 2931 (1972).

⁸See N. F. Mott, *The Metal-Insulator Transition* (Barnes and Noble, New York, 1974).

⁹G. F. Imbusch, *Phys. Rev.* **153**, 326 (1967).

¹⁰I. Y. Gerlovin, *Fiz. Tverd. Tela* **16**, 606 (1974) [*Sov. Phys. Solid State* **16**, 397 (1974)].

¹¹J. Heber, *Phys. Status Solidi (b)* **48**, 319 (1971).

¹²This range of c is fortunately still low enough so that one does not run into possibly more complex energy-transfer processes described by J. C. Murphy, L. C. Aamodt, and C. K. Jen, *Phys. Rev. B* **9**, 2009 (1974).

¹³R. Orbach, *Phys. Lett.* **48A**, 417 (1974).

¹⁴L. A. Riseberg, *Phys. Rev. A* **7**, 671 (1973).

COMMENTS

Possible Effects of Decays of Charmed-Particle Resonances

S. Nussinov*

Institute for Advanced Study, Princeton, New Jersey 08540

(Received 7 October 1975)

Under the assumption that production of the charmed vector meson D^* is important in the charm threshold region, the soft cascade pion (photon) from $D^* \rightarrow D\pi$ ($D^* \rightarrow D\gamma$) for $M_{D^*} - M_D > M_\pi$ ($M_{D^*} - M_D < M_\pi$) could serve as a very useful clue for charmed particles. Also the pions produced in e^+e^- collisions together with (strong-interaction-stable) charmed particles must obey energy equipartition. This strongly suggests other new heavy-quark thresholds and/or heavy-lepton production.

The discovery of even-charge-conjugation states in $\psi \rightarrow \gamma\chi$ decays^{1,2} and of the $\eta_c(2.85 \text{ GeV})$ ³ strongly suggest that ψ spectroscopy is that of a fermion-antifermion system. If the structure in $\sigma_{\text{tot}}(e^+e^- \rightarrow \text{hadrons})$ in the region $4 \leq W \leq 4.6$ GeV reflects $c\bar{c}$ continuum states decaying into charmed-particle pairs, many such $\bar{c}q$ ($q = u, d, s$) composites have already been produced at SPEAR and DESY. The failure to find charmed particles there (and elsewhere) is attributed to multibody decays and to the possible almost simultaneous onset of a heavy-lepton-pair threshold⁴ which tends to reverse the charmed-particle signal in the K/π ratio.⁵ The small mass difference between D^* (1^-) and D ,⁶ the corresponding 0^- state, leads to soft π and γ emissions for $\Delta \equiv M_{D^*} - M_D > m_\pi$ and $\Delta < m_\pi$, respectively. The possible implications, particularly of the $\Delta > 0$ case, for charmed-particle searches are discussed below.

Simple potentiallike models for $\bar{c}c$ bound states

tend to predict $\psi - \eta_c$ mass differences much smaller than the observed value of 250 MeV. The presumably short-range spin-spin forces which cause $^3S-^1S$ splittings are likely to be less effective in the more extended ($\bar{c}q$) systems D and D^* than in the ψ and η_c systems which are composed of two heavy quarks. Thus it is expected that $\Delta = m_{D^*} - m_D \leq m_\psi - m_{\eta_c}$ and in the following I will assume $\Delta \leq 200$ MeV. On the other hand comparison with the larger light-quark system (i.e., the ordinary mesons) suggests that $(m_{D^*})^2 - (m_D)^2 \geq m_{K^*}^2 - m_K^2$. Thus for $m_{D^*} \approx 2$ GeV as indicated by the large rise in R at $W \approx 4$ GeV we find $\Delta \geq 0.14 \approx m_\pi$.

Specific model calculations^{7,8} predict almost complete dominance of the $D^*\bar{D}^*$ mode in the charm threshold region. Even if the detailed prediction of a huge jump ($\delta R \approx 3$) in R over a very small (10–20 MeV) range due to $D^*\bar{D}^*$ is not verified experimentally I believe the qualitative result that $D^*\bar{D}^*$ states are important just at the